Journal of Materials Chemistry C

Accepted Manuscript

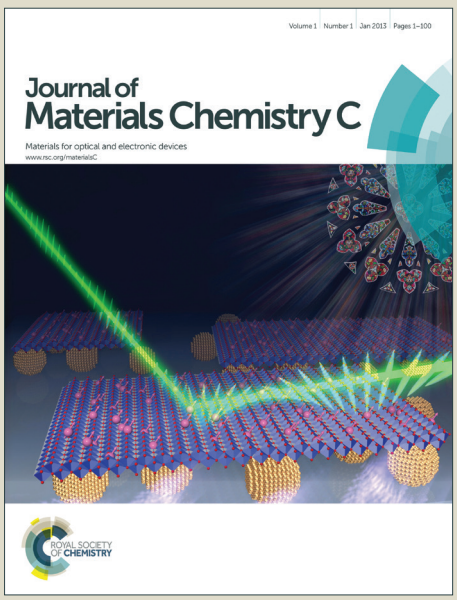

ROYAL SOCIETY OF CHEMISTRY

www.rsc.org/materialsC

Journal Name

RSCPublishing

ARTICLE

D-A-π-A featured sensitizers by modification of auxiliary acceptor for preventing "trade-off" effect†

Cite this: DOI: 10.1039/x0xx00000x

Haibo Zhu,[a] Bo Liu,*[b] Jingchuan Liu,[a] Weiwei Zhang,[a] and Wei-Hong Zhu*[a]

Received 00th January 2012,
Accepted 00th January 2012

DOI: 10.1039/x0xx00000x

www.rsc.org/

Four D-A-π-A motif organic sensitizers (**IQ9**, **IQ10**, **IQ11** and **IQ12**) in absence or presence of thiophene substituents grafted on the auxiliary acceptor of quinoxaline unit have been developed for dye sensitized solar cells (DSSCs). Upon changing the π-linker from benzene to thiophene, **IQ10** increases by around 2-fold in photocurrent (J_{sc}), and decreases by 52 mV in photovoltage (V_{oc}) than that of **IQ9**. It is attributed that, compared with the benzene linker, the thiophene conjugated bridge in dye **IQ10** induces small twist in molecular planarity, thus resulting in the high light-harvesting capability (*beneficial to* J_{sc}) and high charge recombination (*unbeneficial to* V_{oc}). To prevent this "trade-off" effect between photocurrent and photovoltage, the building block of 2,3-dithiophenylquinoxaline as auxiliary unit is specifically incorporated, which brings forth several advantages such as distinctly extending the lighting-harvesting region, increasing molar absorption coefficiencies, and blocking the dye self-aggregation to reduce charge recombination. Remarkably, dye **IQ12** exhibits a beneficial balance between J_{sc} (17.97 mA cm^{-2}) and V_{oc} (715 mV), along with a promising photovoltaic efficiency of 8.76%, much better than the corresponding dyes **IQ9** (2.91%), **IQ10** (7.75%) and **IQ11** (6.56%). As demonstrated, the two twisted thiophene groups grafted onto the quinoxaline unit facilitates the resulting compact sensitizer layer to effectively overcome the charge recombination drawbacks in V_{oc} arising from the thiophene π-bridge linker, providing a rationally molecular engineering to pursue the synergistic enhancement in the photocurrent and photovoltage for high efficient organic sensitizers.

1 Introduction

Dye-sensitized solar cells (DSSCs) have attracted great attention due to high achievable efficiencies in low cost and easy fabrication.[1,2] As a key component, the light-harvesting sensitizer takes responsible for the conversion from photons to electrons, affecting short-circuit photocurrent (J_{sc}) and open-circuit photovoltage (V_{oc}) to a considerable extent.[3] More importantly, there always exists a unpreferable "trade-off" effect between photocurrent and photovoltage, suggesting that any unilateral effort to enhance one side may cause a undesirable decrease to the other side.[4] As a consequence, high photovoltaic conversion efficiency (PCE) can be achieved only when keeping the photocurrent and photovoltage in good balance.[5]

In the traditional donor-π-acceptor (D-π-A) organic sensitizers, the π-bridge linker can greatly affect the light-harvesting of dyes and charge recombination process in cell devices, bringing forth the different behaviours in J_{sc} and V_{oc}.[6] Up to date, many efforts have been devoted to optimize the π-bridge linker to obtain both high J_{sc} and V_{oc}.[7] As the candidates of π-bridge linker, the units of thiophene and benzene have been widely exploited in many pure organic dyes.[8] Generally, the thiophene bridge results in high J_{sc} due to the good molecular conformation between thiophene unit and donor part, along with broad light response. However, the corresponding V_{oc} is relatively lower than those of using benzene unit as the π-bridge. In contrast, the V_{oc} with use of benzene bridge is always increased due to the slow charge recombination rate, but the light response becomes sharply narrowed, leading to a relatively low J_{sc}.[7,8] Accordingly, there is still much room to shed light on an optimal π-bridge linker to prevent the unbeneficial "trade-off" effect. In our previous work, quinoxaline unit was incorporated as additional acceptor in D-A-π-A motif organic sensitizers.[9-12] Through incorporating the auxiliary acceptor into molecular skeleton, the dye light-harvesting capability was distinctly enhanced. With this in mind, herein we further reported four organic sensitizers (**IQ9**, **IQ10**, **IQ11** and **IQ12**) bearing substituted or non-substituted

quinoxaline as the auxiliary acceptor, especially focusing on the synergistic enhancement in J_{sc} and V_{oc}.

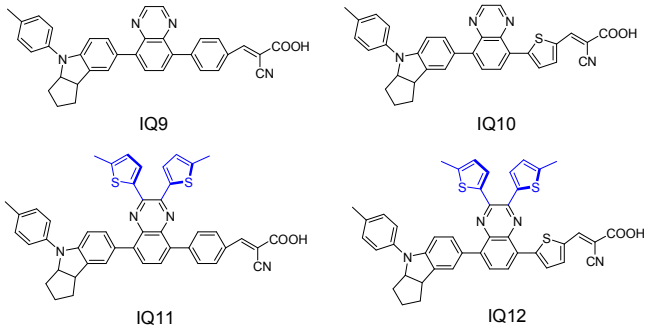

Fig. 1 Chemical structures of D-A-π-A motif sensitizers **IQ9**, **IQ10**, **IQ11** and **IQ12** in absence or presence of thiophene substituents grafted on the auxiliary acceptor of quinoxaline unit.

2 Experimental

2.1 Characterization

^{1}H and ^{13}C NMR spectra were recorded on a Bruker AM 400 spectrometer with tetramethylsilane (TMS) as an internal standard. The UV−vis absorption spectra were recorded with a Varian Cary 100 spectrophotometer. High resolution mass spectrometry (HRMS) was performed using a Waters LCT Premier XE spectrometer. Cyclic voltammograms were performed with a Versastat II electrochemical workstation (Princeton Applied Research) using a normal three-electrode cell with a Pt wire counter electrode, regular calomel reference electrode in a saturated KCl solution, and the working electrode is connected with the TCO glass which deposited the dye-coated TiO_2 film. An amount of 0.1 M tetrabutylammonium hexafluorophosphate ($TBAPF_6$) was used as the supporting electrolyte in CH_2Cl_2.

2.2 Fabrication of DSSCs and photovoltaic characterization

Working electrodes (12 μm nanocrystalline TiO_2 electrodes with a 5 μm scattering layer) were prepared and modified following the reported procedure.[13] A dye solution of sensitizers with a 3×10^{-4} M concentration in 3:7 (v/v) $CHCl_3$/EtOH was used to uptake the dye onto TiO_2 film for 40 h. The counter electrodes were prepared by depositing the Pt catalyst on the cleaned FTO glass by coating with a drop of H_2PtCl_6 solution (50 mM in ethanol solution) with the heat treatment at 500 °C for 30 min. The two electrodes were sandwiched using a 40 μm thick Surlyn spacer and sealed by heating the polymer frame. In this work, 0.6 M 1,2-dimethyl-3-propylimidazolium iodide (DMPII), 0.05 M I_2, 0.1 M LiI, and 0.5 M TBP in acetonitrile were used as the redox electrolyte. The photocurrent density−voltage (I−V) of sealed solar cells was measured under irradiation with a solar simulator (WXS-155S-10) at AM 1.5 illumination (light intensities: 100 mW cm^{-2}). Monochromatic IPCE was measured with monochromatic incident light of 1×10^{16} photons cm^{-2} under 100 mW cm^{-2} in director current mode measurements, which were made on a CEP-2000 system (Bunkoh-Keiki Co. Ltd.).

2.3 Intensity modulated photovoltage spectroscopy (IMVS), charge extraction method (CEM) and electrochemical impedance spectroscopy (EIS)

The IMVS spectra were measured at an open-circuit condition, based on a monochromatic illumination (446 nm) controlled by Labview system, to obtain the photovoltaic response induced by the modulated light.[14] The modulated light was driven with a 10% AC perturbation current superimposed on a DC current in a frequency range from 0.1 to 10^6 Hz. The charge extraction method (CEM) was performed with the same monochromatic light source.[15] The solar cell was illuminated at an open-circuit condition for 5 s to attain a steady state and then the light source was switched off. The charge extraction was calculated by integration of the transient current detected when the laser illumination was turned off and the DSSC was simultaneously stepped from open-circuit to short-circuit. The electrochemical impedance spectra (EIS) were obtained under one sun illumination with a potentiostat (Solartron1287) equipped with a frequency response analyzer (Solartron1255B) under a frequency ranging from 10^{-1} to 10^6 Hz.

2.4 Materials and Synthesis

The starting materials of 3,6-dibromobenzene-1,2-diamine (**1**),[16] 1,2-bis(5-methylthiophen-2-yl)ethane-1,2-dione (**2**)[17] and bromo-substituted indoline (**3**)[18] were prepared according to the established references. Glyoxal, (4-formylphenyl)boronic acid, (5-formylthiophen-2-yl)boronic acid, cyanoacetic acid were purchased from *J&K* Scientific, Ltd. Tetrahydrofuran (THF) was predried over 4 Å molecular sieves and distilled under argon atmosphere from sodium benzophenone ketyl immediately prior to use. All other regents and solvents were purchased as analytical grade from Sinopharm Chemical Reagent Co., Ltd and used as received without further purification.

Journal Name RSCPublishing

ARTICLE

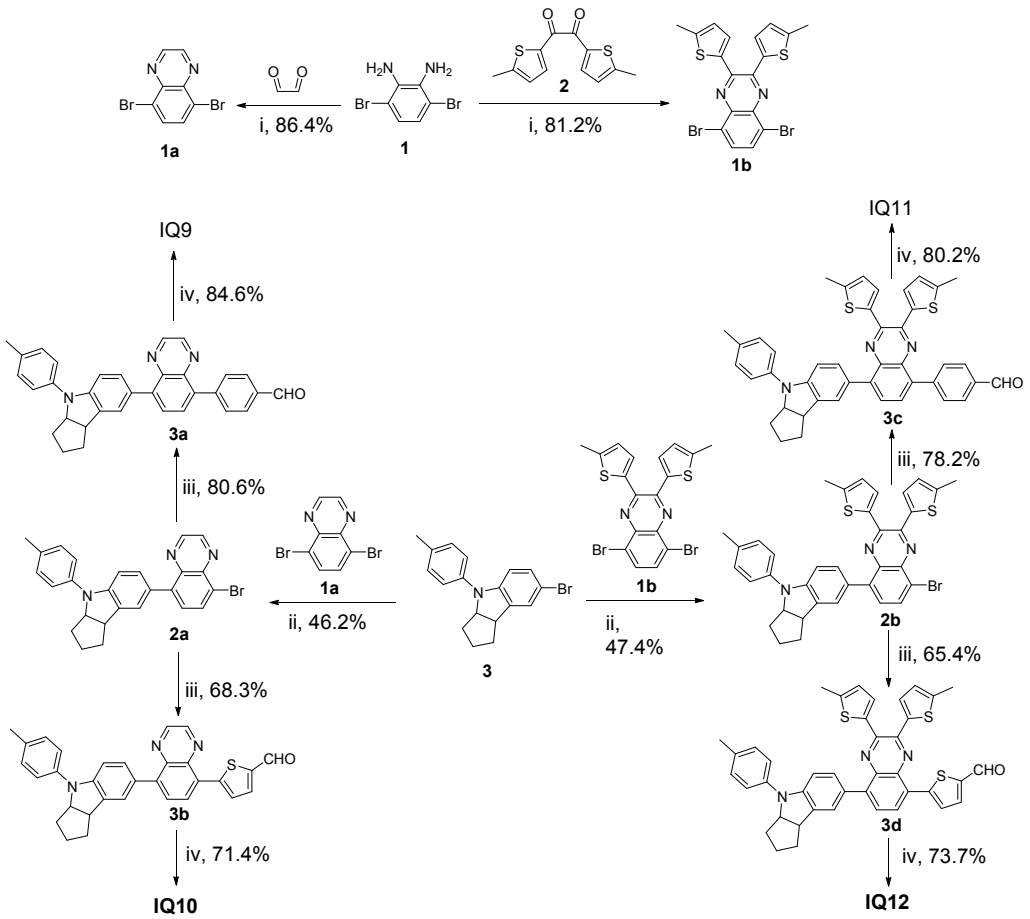

(i) acetic acid, 40 °C, 6 h; (ii) n-BuLi, -78 °C, THF; $B(OCH_3)_3$; $Pd(PPh_3)_4$, K_2CO_3, 80 °C, 8 h; (iii) $Pd(PPh_3)_4$, K_2CO_3, THF, reflux for 7 h; (iv) cyanoacetic acid, piperidine, acetonitrile, reflux for 7 h.

Scheme 1 Synthetic routes to quinoxaline-based D-A-π-A motif sensitizers **IQ9**, **IQ10**, **IQ11** and **IQ12**.

Synthesis of compound 1a. A mixture of glyoxal (5 mL, 40 wt% solution in H_2O), acetic acid (70 mL), 3,6-dibromobenzene-1,2-diamine (3 g, 11.28 mmol), and was stirred at 40 °C for 6 h. The crude product was filtered, and then purified by recrystallization with alcohol. It was obtained as yellowish needle solid 2.8 g, yield 86.4%. ^{1}H NMR (400 MHz, $CDCl_3$, ppm): δ 9.02 (s, 2 H), 8.00 (s, 2 H). ^{13}C NMR (100 MHz, $CDCl_3$, ppm): δ 146.07, 141.57, 133.75, 124.00.

Synthesis of compound 1b. Compound **1b** was obtained as a yellowish solid by similar procedure to that for **1a**, yield 81.2%. ^{1}H NMR (400 MHz, $CDCl_3$, ppm): δ 7.78 (s, 2 H), 7.40 (d, J = 3.7 Hz, 2 H), 6.71 (dd, J_1 = 3.7 Hz, J_2 = 1.0 Hz, 2 H), 2.57 (s, 6 H). ^{13}C NMR (100 MHz, $CDCl_3$, ppm): δ 147.09, 145.88, 138.64, 138.48, 132.63, 130.52, 126.22, 122.89, 15.69. HRMS–ESI (m/z): $[M + H]^+$ Calcd. for ($C_{18}H_{13}Br_2N_2S_2$), 478.8887, found:478.8886.

Synthesis of compound 2a. To a solution of bromo-substituted indoline (1.41 g, 4.29 mmol) in dry THF (20 mL) in a dried schlenk tube was added *n*-BuLi (2 mL, 4.8 mmol) in hexane dropwise at -78 °C, under Argon in dark. After stirring for 2 h at this temperature, $B(OCH_3)_3$ (580 mg, 5.58 mmol) was added slowly to this solution. The reaction mixture was stirred at the same temperature for 4 h, then gradually warmed up to room temperature and used for the next Suzuki coupling reaction without purification. In a three-neck round-bottom flask was dissolved **1a** in THF (50 mL), an aqueous solution of 2 M K_2CO_3 and $Pd(PPh_3)_4$ (80 mg, 0.07 mmol) were added. After the solution was heated at 80 °C, the unpurified mixture

prepared above was added slowly. The reaction mixture was stirred for an additional 8 h. After cooling, water was added and the reaction mixture was extracted with CH_2Cl_2. The combined organic layer was washed with brine, dried over anhydrous Na_2SO_4, and evaporated under reduced pressure. The crude product was purified by column chromatography (CH_2Cl_2 / PE = 1 / 4) on silica gel to yield an orange solid as the desired product, yield 46.2%. ^{1}H NMR (400 MHz, $CDCl_3$, ppm): δ 8.96 (s, 1 H), 8.92 (s, 1 H), 8.12 (d, J = 7.9 Hz, 1 H), 7.67 (d, J = 7.9 Hz, 1 H), 7.43 (s, 1 H), 7.35 (d, J = 8.2 Hz, 1 H), 7.24 (d, J = 8.4 Hz, 2 H), 7.17 (d, J = 8.2 Hz, 2 H), 7.01 (d, J = 8.3 Hz, 1 H), 4.90-4.82 (m, 1 H), 3.97-3.87 (m, 1 H), 2.34 (s, 3 H), 2.10-2.01 (m, 1 H), 2.00-1.88 (m, 2 H), 1.87-1.75 (m, 1 H), 1.73-1.56 (m, 2 H). ^{13}C NMR (100 MHz, $CDCl_3$, ppm): δ 148.22, 144.88, 144.66, 142.06, 141.73, 140.93, 134.90, 133.43, 131.51, 130.10, 129.82, 129.77, 127.01, 126.99, 121.44, 120.20, 107.07, 69.17, 45.39, 35.09, 33.70, 24.52, 20.80. HRMS–ESI (*m/z*): $[M + H]^+$ calcd. for ($C_{26}H_{23}N_3{}^{79}Br$), 456.1075, found: 456.1073. $[M + H]^+$ calcd. for ($C_{26}H_{23}N_3{}^{81}Br$), 458.1055, found: 458.1057.

Synthesis of compound 2b. 2b was obtained as red solid by similar procedure to that for **2a**, yield 47.4%. ^{1}H NMR (400 MHz, $CDCl_3$, ppm): δ 7.94 (d, J = 8.0 Hz, 1 H), 7.61 (s, 1 H), 7.56 (d, J = 8.0 Hz, 1 H), 7.45 (dd, J_1 = 8.3 Hz, J_2 = 1.8 Hz, 1 H), 7.4 (d, J = 3.6 Hz, 1 H), 7.30 (d, J = 3.6 Hz, 1 H), 7.26 (d, J = 8.5 Hz, 2 H), 7.18 (d, J = 8.3 Hz, 2 H), 7.04 (d, J = 8.3 Hz, 1 H), 6.70 (dd, J_1 = 3.7 Hz, J_2 = 2.2 Hz, 1 H), 6.64 (dd, J_1 = 3.6 Hz, J_2 = 1.0 Hz, 1 H), 4.89-4.82 (m, 1 H), 4.39-3.89 (m, 1 H), 2.57 (s, 3 H), 2.51 (s, 3H), 2.35 (s, 3 H), 2.16-2.06 (m, 2 H), 2.04-1.92 (m, 1 H), 1.90-1.78 (m, 1 H), 1.75-1.59 (m, 2 H). ^{13}C NMR (100 MHz, $CDCl_3$, ppm): δ 147.85, 145.52, 145.19, 144.94, 144.66, 140.47, 139.82, 139.72, 139.40, 138.42, 137.98, 134.51, 132.72, 131.25, 130.06, 129.82, 129.79, 129.67, 128.70, 127.74, 127.26, 126.02, 125.93, 120.57, 119.95, 107.24, 69.19, 45.58, 35.00, 33.86, 24.59, 20.83, 15.69, 15.63. HRMS–ESI (*m/z*): $[M + H]^+$ calcd. for ($C_{36}H_{31}{}^{79}BrN_3S_2$), 648.1143, found: 648.1147. $[M + H]^+$ calcd. for ($C_{36}H_{31}{}^{81}BrN_3S_2$), 650.1122, found: 650.1132.

Synthesis of compound 3a. In a three-neck round-bottom flask was dissolved **2a** (300 mg, 0.65 mmol) in THF (50 mL), a aqueous solution of 2 M K_2CO_3 (15 mL), 4-formylphenylboronic acid (197 mg, 1.31 mmol) and $Pd(PPh_3)_4$ (20 mg, 0.017 mmol) were added. The mixture was refluxed for 8 h under argon. After cooling, water was added and the reaction mixture was extracted with CH_2Cl_2. The combined organic layer was washed with brine, dried over anhydrous Na_2SO_4, and evaporated under reduced pressure. The crude product was purified by column chromatography (CH_2Cl_2 / PE = 1 / 1) on silica gel to yield an orange solid as the desired product, yield 80.6%. ^{1}H NMR (400 MHz, $CDCl_3$, ppm): δ 10.12 (s, 1 H), 8.93 (s, 1 H), 8.86 (s, 1 H), 8.03 (d, J = 7.9 Hz, 2 H), 7.93-7.84 (m, 4 H), 7.51 (s, 1 H), 7.44 (d, J = 8.2, 1 H), 7.25 (d, J = 5.4 Hz, 2 H), 7.18 (d, J = 8.2 Hz, 2 H), 7.04 (d, J = 8.2 Hz, 1 H), 4.91-4.83 (m, 1H), 3.99-3.89 (m, 1 H), 2.35 (s, 3 H), 2.14-2.03 (m, 1 H), 2.01-1.89 (m, 2 H), 1.89-1.76 (m, 1 H), 1.74-1.59 (m, 2 H). ^{13}C NMR (100 MHz, $CDCl_3$, ppm): δ 192.16, 148.19, 145.01, 144.24, 144.20, 142.12, 141.28, 141.16, 140.30, 137.51, 135.32, 134.91, 131.48, 131.37, 130.53, 130.21, 129.81, 129.52, 129.26, 127.66, 127.16, 120.20, 107.15, 69.21, 45.48, 35.13, 33.77, 24.59, 20.84. HRMS–ESI (*m/z*): $[M + H]^+$ calcd. for ($C_{33}H_{28}N_3O$), 482.2232, found: 482.2230.

Synthesis of compound 3b. The Suzuki coupling reaction of **2a** with 5-formylthiophen-2-yl-2-boronic acid was carried out in a similar manner to that for **3a**. The crude product was purified by column chromatography (CH_2Cl_2 / PE = 1 / 1) to yield **3b** as a red solid, yield 68.3%. ^{1}H NMR (400 MHz, $CDCl_3$, ppm): δ 9.99 (s, 1 H), 8.93 (d, J = 1.6 Hz, 1 H), 8.94 (d, J = 1.6 Hz, 1 H), 8.23 (d, J = 7.8 Hz, 1 H), 7.88 (d, J = 3.7 Hz, 1 H), 7.86 (d, J = 6.2 Hz, 1 H), 7.82 (d, J = 4.0 Hz, 1 H), 7.51 (s, 1 H), 7.43 (dd, J_1 = 8.3, J_2 =1.6 Hz, 1 H), 7.25 (d, J = 9.3 Hz, 2 H), 7.17 (d, J = 8.4 Hz, 2 H), 7.02 (d, J = 8.3 Hz, 1 H), 4.91-4.83 (m, 1 H), 3.97-3.89 (m, 1 H), 2.35 (s, 3 H), 2.14-2.01 (m, 1 H), 2.00-1.89 (m, 2 H), 1.88-1.76 (m, 1 H), 1.73-1.61 (m, 2 H). ^{13}C NMR (100 MHz, $CDCl_3$, ppm): δ 183.56, 148.57, 144.75, 144.37, 143.43, 142.46, 141.24, 140.16, 136.30, 135.80, 135.14, 134.96, 131.64, 130.34, 129.81, 129.55, 129.17, 128.68, 128.32, 127.14, 127.04, 120.33, 107.12, 69.25, 45.43, 35.14, 33.71, 24.54, 20.83. HRMS–ESI (*m/z*): $[M + H]^+$ calcd. for ($C_{31}H_{26}N_3OS$), 488.1797, found: 488.1797.

Synthesis of compound 3c. Compound **3c** was obtained as a red solid by similar procedure to that for **3a** but with **2b** instead of **2a**, yield 78.2%. ^{1}H NMR (400 MHz, $CDCl_3$, ppm): δ 10.13 (s, 1 H), 8.04 (d, J = 8.5 Hz, 2 H), 8.00 (d, J = 8.5 Hz, 2 H), 7.79 (s, 2 H), 7.69 (s, 1 H), 7.53 (dd, J_1 = 8.3 Hz, J_2 = 1.8 Hz, 1 H), 7.35 (d, J = 3.7 Hz, 1 H), 7.34 (d, J = 3.7 Hz, 1 H), 6.27 (d, J = 8.4 Hz, 2 H), 7.19 (d, J = 8.4 Hz, 2 H), 7.07 (d, J = 8.2 Hz, 1 H), 6.73 (dd, J_1 = 2.4, J_2 =1.2 Hz, 2 H), 4.91-4.83 (m, 1H), 3.99-3.90 (m, 1 H), 2.52 (s, 6 H), 2.36 (s, 3 H), 2.20-2.05 (m, 2 H), 2.03-1.93 (m, 1 H), 1.91-1.79 (m, 1 H), 1.77-1.61 (m, 2 H). ^{13}C NMR (100 MHz, $CDCl_3$, ppm): δ 192.50, 147.76, 144.81, 144.68, 144.47, 144.28, 140.48, 140.23, 140.16, 137.80, 137.68, 135.58, 135.01, 134.49, 131.53, 131.24, 130.18, 130.00, 129.79, 129.47, 129.31, 128.29, 127.87, 127.71, 125.96, 125.85, 119.95, 107.25, 69.20, 45.61, 35.02, 33.87, 24.61, 20.83, 15.71, 15.64. HRMS–ESI (*m/z*): $[M + H]^+$ Calcd. for ($C_{43}H_{36}N_3OS_2$), 674.2300, found: 674.2296.

Synthesis of compound 3d. Compound **3d** was obtained as a red solid by similar procedure to that for **3a**, yield 65.4%.^{1}H NMR (400 MHz, $CDCl_3$, ppm): δ 9.99 (s, 1 H), 8.09 (d, J = 8.0 Hz, 1 H), 7.93 (d, J = 4.0 Hz, 1 H), 7.83 (d, J = 4.1 Hz, 1 H), 7.75 (d, J = 7.9 Hz, 1 H), 7.69 (s, 1 H), 7.53 (dd, J_1 = 8.3 Hz, J_2 = 1.9 Hz, 1 H), 7.45 (d, J = 3.7 Hz, 1 H), 7.32 (d, J = 3.7 Hz, 1 H), 6.27 (d, J = 8.0 Hz, 2 H), 7.19 (d, J = 8.1 Hz, 2 H), 7.06 (d, J = 8.3 Hz, 1 H), 6.73 (dd, J_1 = 3.7, J_2 = 1.3 Hz, 1 H), 6.65 (dd, J = 3.8, 1.3 Hz, 1 H), 4.93-4.84 (m, 1 H), 3.98-3.91 (m, 1 H), 2.61 (s, 3 H), 2.52 (s, 3 H), 2.36 (s, 3 H), 2.18-2.08 (m, 2 H), 2.04-

1.93 (m, 1 H), 1.91-1.79 (m, 1 H), 1.77-1.64 (m, 2 H). ^{13}C NMR (100 MHz, $CDCl_3$, ppm): δ 183.42, 149.32, 148.11, 145.23, 144.84, 144.62, 144.53, 144.19, 140.63, 140.36, 140.14, 139.25, 137.73, 136.84, 136.00, 134.57, 134.47, 131.42, 130.30, 129.82, 129.65, 128.29, 128.13, 128.07, 127.88, 127.40, 127.01, 126.08, 125.96, 120.09, 107.24, 69.25, 45.59, 35.05, 33.83, 24.60, 20.85, 15.82, 15.66. HRMS–ESI (*m/z*): $[M + H]^+$ Calcd. for ($C_{41}H_{34}N_3OS_3$), 680.1864, found: 680.1862.

Synthesis of IQ9. A mixture of aldehyde **3a** (120 mg, 0.25 mmol) and cyanoacetic acid (176 mg, 2.07 mmol) in acetonitrile (30 mL) was heated to reflux in the presence of piperidine (0.5 mL) for 7 h under argon. After cooling, the mixture was diluted with CH_2Cl_2 (50 mL). The combined organic layer was washed with water and brine, dried over Na_2SO_4, and evaporated under reduced pressure. The crude product was purified by column chromatography (CH_2Cl_2 / MeOH = 20 / 1) on silica gel to yield the product as a red solid 116 mg, yield 84.6%. ^{1}H NMR (400 MHz, DMSO, ppm): δ 8.91 (d, J = 6.4 Hz, 2 H), 7.97 (d, J = 7.6 Hz, 1 H), 7.90 (d, J = 6.7 Hz, 1 H), 7.86 (d, J = 5.2 Hz, 1 H), 7.78 (d, J = 7.8 Hz, 1 H), 7.67 (d, J = 8.2 Hz, 1 H), 7.48 (d, J = 7.8 Hz, 1 H), 7.45 (s, 1 H), 7.42-7.28 (m, 2 H), 7.19 (d, J = 8.2 Hz, 2 H), 7.13 (d, J = 8.1 Hz, 2 H), 6.90 (d, J = 8.2 Hz, 1 H), 4.89-4.76 (m, 1 H), 3.89-3.77 (m, 1 H), 2.22 (s, 3 H), 2.06-1.88 (m, 1 H), 1.83-1.65 (m, 3 H), 1.63-1.51 (m, 1 H), 1.46-1.29 (m, 1 H). ^{13}C NMR (100 MHz, DMSO, ppm): δ 146.84, 144.74, 144.62, 144.60, 140.26, 140.10, 139.87, 138.56, 137.66, 137.01, 134.33, 131.20, 130.91, 130.47, 130.23, 130.12, 129.74, 129.14, 127.78, 127.65, 127.07, 126.97, 124.25, 119.38, 118.76, 106.50, 68.24, 44.61, 34.78, 33.21, 24.00, 20.35. HRMS–ESI (*m/z*): $[M + H]^+$ calcd. for ($C_{36}H_{29}N_4O_2$), 549.2291, found: 549.2291.

Synthesis of IQ10. IQ10 was obtained as purple powder in a similar way as **IQ9**, yield 71.4%. ^{1}H NMR (400 MHz, DMSO, ppm): δ 9.05 (d, J = 3.8 Hz, 2 H), 8.47 (d, J = 8.0 Hz, 1 H), 8.29 (s, 1 H), 8.10 (d, J = 4.0 Hz, 1 H), 7.92 (m, 2 H), 7.54 (s, 1 H), 7.44 (m, 1 H), 7.26 (d, J = 8.4 Hz, 2 H), 7.19 (d, J = 8.3 Hz, 2 H), 6.95 (d, J = 8.4 Hz, 1 H), 4.95-4.85 (m, 1 H), 3.95-3.84 (m, 1 H), 2.29 (s, 3 H), 2.10-1.93 (m, 1 H), 1.90-1.72 (m, 3 H), 1.70-1.58 (m, 1 H), 1.50-1.35 (m, 1 H). ^{13}C NMR (100 MHz, DMSO, ppm): δ 163.77, 147.15, 144.96, 144.07, 140.68, 140.17, 139.70, 138.81, 138.65, 134.41, 130.65, 130.33, 130.23, 129.75, 129.14, 129.04, 128.31, 127.55, 127.24, 127.10, 124.25, 119.51, 106.49, 68.28, 44.57, 34.81, 33.16, 23.98, 20.37. HRMS–ESI (*m/z*): $[M + H]^+$ calcd. for ($C_{34}H_{27}N_4O_2S$), 555.1855, found: 555.1858.

Synthesis of IQ11. IQ11 was obtained as purple powder in a similar way as **IQ9**, yield 80.2%. ^{1}H NMR (400 MHz, THF-d_8, , ppm): δ 8.35 (s, 1 H), 8.19 (d, J = 8.1 Hz, 2 H), 8.01 (d, J = 8.1 Hz, 2 H), 7.88 (d, J = 7.6 Hz, 1 H), 7.82 (d, J = 7.6 Hz, 1 H), 7.68 (s, 1 H), 7.49 (d, J = 8.4 Hz, 1 H), 7.31 (m, 2 H), 7.25 (d, J = 8.2 Hz, 2 H), 7.14 (d, J = 8.2 Hz, 2 H), 6.99 (d, J = 8.3 Hz, 1 H), 6.67 (d, J = 3.1 Hz, 2 H), 4.95-4.85 (m, 1 H), 4.00-3.89 (m, 1 H), 2.49 (s, 6 H), 2.30 (s, 3 H), 2.16-2.07 (m, 2 H), 2.00-1.90 (m, 1 H), 1.89-1.78 (m, 1 H), 1.68-1.58 (m, 2 H). ^{13}C NMR (100 MHz, THF-d_8, ppm): δ 162.95, 153.62, 147.68, 144.40, 144.21, 144.02, 143.31, 140.58, 140.42, 140.31, 137.75, 137.65, 135.51, 134.21, 131.37, 130.77, 130.26, 129.79, 129.48, 129.11, 128.97, 128.19, 127.72, 125.69, 125.65, 119.72, 115.47, 106.79, 103.11, 69.00, 45.57, 34.99, 33.66, 19.88, 14.45. HRMS–ESI (*m/z*): $[M + H]^+$ Calcd. for ($C_{46}H_{37}N_4O_2S_2$), 741.2358, found: 741.2362.

Synthesis of IQ12. IQ12 was obtained as purple powder in a similar way as **IQ9**, yield 73.7%. ^{1}H NMR (400 MHz, DMSO, ppm): δ 8.20 (s, 1 H), 8.14 (d, J = 6.5 Hz, 1 H), 7.91 (s, 1 H), 7.74 (d, J = 3.1 Hz, 1 H), 7.62 (d, J = 6.4 Hz, 1 H), 7.54 (s, 1 H), 7.42 (d, J = 3.0 Hz, 1 H), 7.32 (d, J = 7.4 Hz, 1 H), 7.27-7.11 (m, 5 H), 6.91 (d, J = 8.2 Hz, 1 H), 6.80 (s, 1 H), 6.74 (s, 1 H), 4.93-4.78 (m, 1 H), 3.89-3.75 (m, 1 H), 2.53 (s, 3 H), 2.45 (s, 3 H), 2.29 (s, 3 H), 2.11-1.91 (m, 2 H), 1.89-1.71 (m, 2 H), 1.71-1.56 (m, 1 H), 1.53-1.33 (m, 1 H). ^{13}C NMR (100 MHz, DMSO, ppm): δ 164.20, 146.99, 145.00, 143.93, 143.81, 143.74, 139.66, 139.08, 139.02, 138.66, 138.25, 136.59, 135.52, 134.05, 130.47, 130.16, 129.72, 129.63, 129.46, 128.06, 127.84, 127.69, 127.07, 126.35, 126.23, 119.29, 118.93, 106.47, 68.18, 44.69, 34.60, 33.18, 24.05, 20.37, 15.30, 15.10. HRMS–ESI (*m/z*): $[M + H]^+$ Calcd. for ($C_{44}H_{35}N_4O_2S_3$), 747.1922, found: 747.1919.

3 Results and discussion

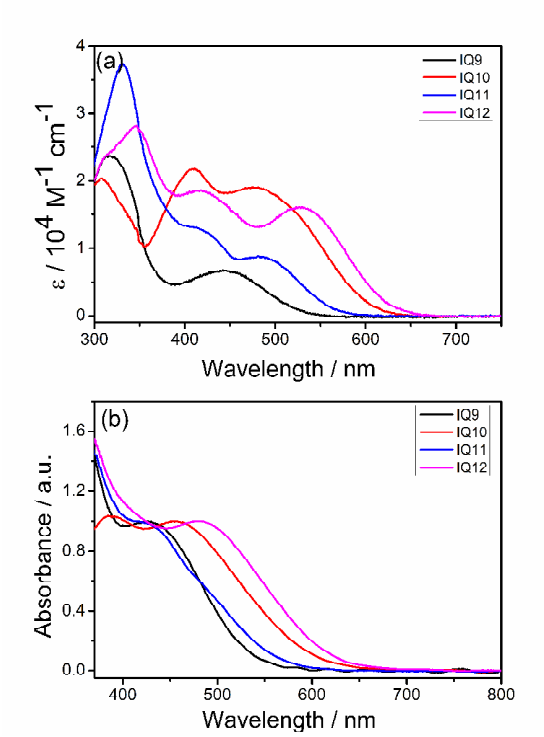

Fig. 2 Absorption spectra of quinoxaline-based sensitizers **IQ9**, **IQ10**, **IQ11** and **IQ12**: (a) in dichloromethane (DCM) and (b) anchored on a transparent 3 μm nanocrystalline TiO_2 film.

As typical D-A-π-A motif dyes, we specifically developed four organic sensitizers (**IQ9**-**IQ12**) bearing substituted or non-substituted quinoxaline as the auxiliary acceptor (Scheme 1). Moreover, we chose phenyl and thienyl group as typical π-bridge for comparison. Indeed, it is well-documented that thiophene moiety is a superiorπ-conjugated linker than phenyl moiety for strong charge-transfer, high carrier-transport and strong light absorption for optoelectronic materials. All these dyes exhibited two or three absorption bands in ultra-visible (UV) region (Fig. 2a), arising from the characteristic π-π transition and intramolecular charge-transfer (ICT). When using thiophene as the π-bridge linker, the ICT bands for dyes **IQ10** (475 nm) and **IQ12** (530 nm) exhibited red-shift with respect to the corresponding benzene-bridged dyes **IQ9** (442 nm) and **IQ11** (481 nm). It can be attributed to the good molecular planarity and small conformation twist.[19] Exactly, the dihedral angles (θ) between quinoxaline and π-bridge linker (Table 1) in **IQ10** and **IQ12** are calculated as 2.5º and 12.7º, respectively, which are much as smaller than that of **IQ9** (41.8º) and **IQ11** (42.5º). Besides the π-bridge, we also found that the modification with auxiliary acceptor has a great effect on the ICT absorption band. That is, the absorption peaks (λ_{max}) of dyes **IQ11** and **IQ12** containing two thiophene grafted-quinoxaline unit (2,3-dithiophenylquinoxaline) appeared at 481 and 530 nm, respectively. Compared with non-substituted-quinoxaline unit, dyes **IQ11** and **IQ12** exhibited 39 and 55 nm in bathochromic shift, respectively. It is suggestive that the building block of 2,3-dithiophenylquinoxaline can effectively extend the absorption wavelength and enhance the solar light utilization. As a matter of fact, the two grafted thiophene groups on the auxiliary quinoxaline acceptor are spatially crowded in their twisted arrangement (Scheme 1), which might exhibit some anti-aggregation effect. Actually, the aggregation behavior on TiO_2 include two aspects of *H*-aggregation (blue shift) and *J*-aggregation (red shift) in absorption. Compared with the absorption band in dichloromethane, the TiO_2 film absorption of **IQ9**, **IQ10**, **IQ11** and **IQ12** exhibited blue shifts by 16, 22, 66 and 51 nm (Fig. 2b), respectively. Obviously, **IQ11** and **IQ12** might predominately prevent the *J*-aggregation to some extent, rather than *H*-aggregation.

Table 1 Photophysical and electrochemical properties of sensitizers **IQ9**, **IQ10**, **IQ11** and **IQ12**.

Dyes	λ_{max} [a] [nm]	ε [a] [M^{-1} cm^{-1}]	λ_{max} [b] [nm]	θ [c] [º]	HOMO [V] [d]	E_{0-0} [e] [V]	LUMO [e] [V]
IQ9	442	6826	426	41.8	0.85	2.30	-1.45
IQ10	411 475	21736 19008	453	2.5	0.86	2.06	-1.20
IQ11	410 481	13350 8907	415	42.5	0.82	2.22	-1.40
IQ12	418 530	18610 16137	479	12.7	0.85	1.99	-1.14

Note: [a]Absorption parameters were obtained in CH_2Cl_2. [b]Absorption parameters were obtained on 3 μm nanocrystalline TiO_2 film. [c]The dihedral angles (θ) between quinoxaline and π-bridge linker were calculated by the Gaussian 09 program using B3LYP method and 6-31G* basis set.[20] [d]The HOMO was obtained in CH_2Cl_2 with ferrocene (0.63 V vs. NHE) as external reference. [e]E_{0-0} values were estimated from the wavelength at 10% maximum absorption intensity for the dye-loaded 3 μm nanocrystalline TiO_2 film. [e]The LUMO was calculated according to LUMO = HOMO – E_{0-0}.

Cyclic voltammetry was also carried out to investigate the influence of different substituents (Fig. S1†). As listed in Table 1, with the same donor part of indoline, all four dyes presented similar HOMO levels around 0.85 V, which were more positive than the redox potential of the I^-/I_3^- redox couple (0.4 V vs NHE), ensuring sufficient driving force to regeneration from oxidized dye molecules. Due to the longer onset wavelength of **IQ10** and **IQ12**, the E_{0-0} values were calculated to be lower than those of **IQ9** and **IQ11**. As a result, the more positive LUMO levels of **IQ10** and **IQ12** were obtained. However, the LUMO levels of four dyes were all more negative than conduction band of TiO_2 (−0.5 V vs NHE). Thus, such slightly difference in energy levels of four dyes would not affect the electron injection and dye regeneration process to a large extent.

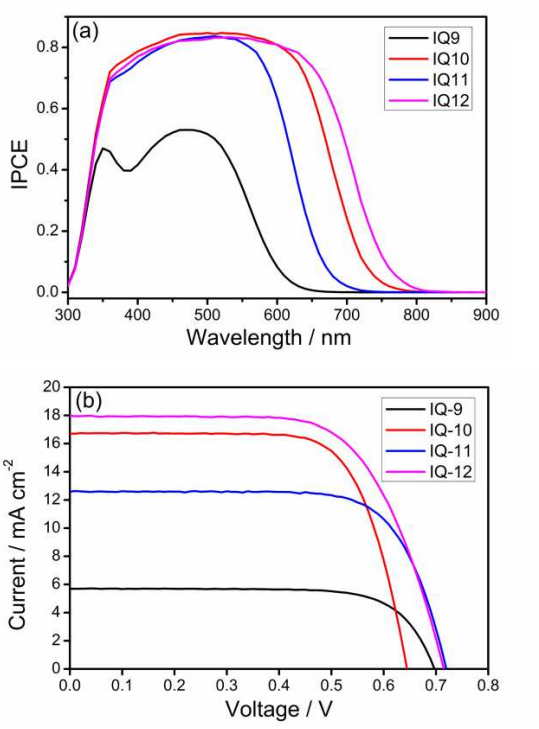

Fig. 3 (a) IPCE and (b) J-V curves of DSSCs sensitized by quinoxaline-based dyes **IQ9**, **IQ10**, **IQ11** and **IQ12** using I^-/I_3^- as the electrolyte.

Fig. 3 shows the photovoltaic performance of DSSCs based on these dyes under standard AM 1.5 irradiation (100 mW cm^{-2}). The detail photovoltaic parameters are collected in Table 2. Obviously, the IPCE onsets for dyes **IQ10** (786 nm) and **IQ12** (815 nm) based on thiophene as the π-bridge linker exhibited red-shift with respect to the corresponding benzene-bridged dyes **IQ9** (660 nm) and **IQ11** (734 nm). Specifically, the low plateau of the IPCE value for **IQ9** (only reached 53%) and its narrow spectral response leaded to the lowest J_{sc} of 5.70 mA cm^{-2}. Through simply alternating the π-bridge linker from benzene to thiophene, the J_{sc} was sharply enhanced by almost two folds from 5.70 mA cm^{-2} (**IQ9**) to 16.72 mA cm^{-2} (**IQ10**). It is well suggestive that the thiophene-bridged linker is beneficial to the IPCE and J_{sc}, which is in exact accordance with the absorption spectra observed for the dye-loaded TiO_2 films (Fig. 2b). It is notable that, in the fabricated devices, the 12 μm nanocrystalline TiO_2 electrodes with a 5 μm scattering layer can greatly shift the onset of the dyes in IPCE.[13] For instance, the onset of **IQ12** in IPCE is greatly shifted to 800 nm when compared to the absorption onset of film on TiO_2 at 650 nm. However, the unpreferable trade-off was observed, that is, the V_{oc} was decreased from 697 mV (**IQ9**) to 645 mV (**IQ10**). Interestingly, when grafting two thiophene substituents onto quinoxaline segment, the V_{oc} of **IQ12** was rebounded to 715 mV, which was even higher than that of **IQ9** (697 mV), and only slightly lower than that of **IQ11** (720 mV). It is the introduction of 2,3-dithiophenylquinoxaline that could effectively overcome the drawbacks in V_{oc} arising from the thiophene π-bridge linker.

As well known, the V_{oc} is defined as the energy difference between the quasi-Fermi level (E_F) of TiO_2 and the Fermi level of the redox couple in the electrolyte.[3b] Considering that the redox couple fabricated in the cells is identical, the difference in V_{oc} for **IQ9**, **IQ10**, **IQ11** and **IQ12** is mainly ascribed to the quasi-Fermi level (E_F) of the mesoporous TiO_2 film, which is related to the conduction-band edge position of TiO_2 and the electron density in TiO_2. Thus, to take insight into the physical origin of V_{oc}, charge extraction method (CEM) and intensity modulated photovoltage spectroscopy (IMVS) were performed (Fig. 4).

As shown in Fig. 4a, all four dyes exhibited approximately linear increase in V_{oc} as a function of the logarithm of electron density and overlapped with each other. At a fixed electron density, four dyes presented similar V_{oc}. It is indicative that DSSCs based on these dyes endow the similar conduction band position, and rule out the conduction band as the main reason to photovoltage.[21] Therefore, we consider that the difference in V_{oc} for these four dyes should be attributed to the electron density in TiO_2, which is associated with the balance between the electron injection and charge recombination process. It is closely related to the electron lifetimes (τ_e) measured by the IMVS method. As shown in Fig. 4b, at a fixed V_{oc}, the electron lifetime of **IQ10** containing thiophene as π-bridge linker was the shortest one among these four dyes. While the π-bridge linker was changed to the benzene unit, the electron lifetime of **IQ9** was sharply increased, indicating that the use of thiophene as the linker would cause serious charge recombination. Remarkably, when the two thiophene substituents were grafted onto the quinoxaline unit the electron lifetimes of **IQ12** almost laid in the same line as **IQ11**, suggesting that the serious charge recombination arising from thiophene linker was effectively prevented by the insertion of sterically twisted 2,3-dithiopheylquinoxaline.

Table 2 Photovoltaic parameters of DSSCs based on dyes **IQ9**, **IQ10**, **IQ11** and **IQ12** obtained by using I^-/I_3^- redox couple[a].

Dyes	J_{sc} / mA cm^{-2}	V_{oc} / mV	*FF*	η
IQ9	5.70 ± 0.12	697 ± 2	0.732 ± 0.003	2.91 ± 0.07
IQ10	16.72 ± 0.33	645 ± 1	0.720 ± 0.009	7.75 ± 0.19
IQ11	12.59 ± 0.17	720 ± 4	0.724 ± 0.004	6.56 ± 0.25
IQ12	17.97 ± 0.15	715 ± 2	0.682 ± 0.027	8.76 ± 0.24

[a]The electrolyte was consisted of 0.6 M 1,2-dimethyl-3-propylimidazolium iodide (DMPII), 0.05 M I_2, 0.1 M LiI, and 0.5 M TBP in acetonitrile. The parameters were obtained from the averaged five devices.

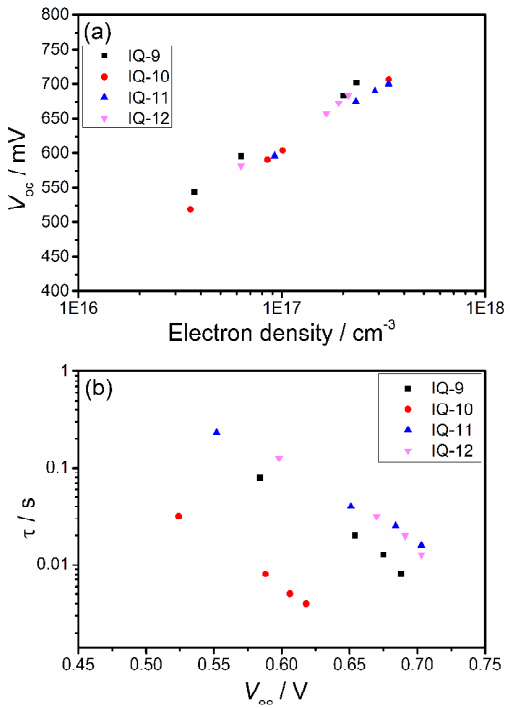

Fig. 4 (a) V_{oc} as a function of electron density and (b) Electron lifetime as a function of V_{oc} for DSSCs sensitized with quinoxaline-based sensitizers **IQ9**, **IQ10**, **IQ11** and **IQ12** measured by CEM and IMVS methods, respectively.

To characterize the detailed interfacial charge transfer process in cell devices, electrochemical impedance spectroscopies (EIS) of all dyes were measured (Fig. 5).[19,22] In the Nyquist diagram, three semicircles from left to right are visible, and represent the impedances of charge transfer on the Pt counter electrode (smaller circles), the charge recombination at TiO_2/dye/electrolyte interface (larger circles), and carrier transport within electrolyte (smaller circles on the right). Similar impedances of the charge transfer on Pt counter electrode and carrier transport within electrolyte could be easily observed. However, the diameter of the second semicircle, corresponding to the impedance of the charge recombination at TiO_2/dye/electrolyte interface, increased in the order of **IQ10** < **IQ9** < **IQ12** < **IQ11**, laying in the same order of the electron lifetime as well as the V_{oc} values. As a result, the building block of 2,3-dithiophenylquinoxaline can effectively prevent the redox mediator from accessing to the TiO_2 surface, and suppress the charge recombination between I_3^- and the injected electron in TiO_2, thus leading to a higher electron lifetime. In this way, the higher V_{oc} value of **IQ12** was observed.

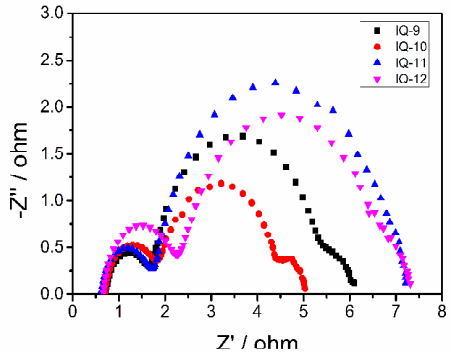

Fig. 5 EIS Nyquist plots for DSSCs sensitized with quinoxaline-based sensitizers **IQ9**, **IQ10**, **IQ11** and **IQ12**.

4 Conclusions

In summary, four D-A-π-A motif organic sensitizers (**IQ9**, **IQ10**, **IQ11** and **IQ12**) have been specifically developed. As demonstrated, the benzene conjugated bridge in dye **IQ9** induces large twist in molecular planarity, thus resulting in the poor light-harvesting capability (unbeneficial to J_{sc}) and lower charge recombination (beneficial to V_{oc}). In contrast, the thiophene conjugated bridge in dye **IQ10** induces small twist in molecular planarity, along with beneficial J_{sc} and unbeneficial V_{oc}. Upon grafting two thiophene groups onto the auxiliary quinoxaline acceptor in molecular skeleton, the resulting building block of 2,3-dithiophenylquinoxaline can distinctly extend the absorption wavelength, increase light-harvesting efficiency, and prevent the dye self-aggregation, thus successfully eliminating the unpreferabe "trade-off" effect between photocurrent and photovoltage. Remarkably, dye **IQ12** exhibited the balance of J_{sc} (17.97 mA cm^{-2}) and V_{oc} (715 mV), along with a promising photovoltaic efficiency of 8.76%, much better than the corresponding dyes **IQ9** (2.91%), **IQ10** (7.75%) and **IQ1** (6.56%). As a consequence, the insertion of 2,3-dithiophenylquinoxaline unit is able to effectively overcome the charge recombination drawbacks in V_{oc} arising from the thiophene π-bridge linker. Our finding affords a promising way to pursue the synergistic enhancement in the photocurrent and photovoltage for high efficient organic sensitizers.

Acknowledgements
This work was supported by NSFC for Creative Research Groups (21421004) and Distinguished Young Scholars (21325625), NSFC/China and the Oriental Scholarship.

Notes and references
[a]*Shanghai Key Laboratory of Functional Materials Chemistry, Key Laboratory for Advanced Materials and Institute of Fine Chemicals, , Collaborative Innovation Center for Coal Based Energy (i-CCE), East China University of Science and Technology, Shanghai 200237, P. R. China. E-mail: whzhu@ecust.edu.cn*
[b]*College of Chemistry and Material Science, Hebei Normal University, No. 20, East Road of Nan Er Huan, Shijiazhuang 050023, P. R. China. E-mail: liubo@mail.hebtu.edu.cn*

Electronic Supplementary Information (ESI) available: Cyclic voltammograms, NMR and Mass spectra. See DOI: 10.1039/b000000x/

1 B. O'Regan and M. Grätzel, *Nature*, 1991, **353**, 737.
2 (*a*) A. Hagfeldt, G. Boschloo, L. Sun, L. Kloo and H. Pettersson, *Chem. Rev.*, 2010, **110**, 6595; (*b*) S. Zhang, X. Yang, Y. Numata and L. Y. Han, *Energy Environ. Sci.*, 2013, **6**, 1443.
3 (*a*) A. Mishra, M. K. R. Fischer and P. Bäuerle, *Angew. Chem. Int. Ed.*, 2009, **48**, 2474; (*b*) Z. Ning, Y. Fu and H. Tian, *Energy Environ. Sci.*, 2010, **3**, 1170; (*c*) J. Yum, E. Baranoff, S. Wenger, M. K. Nazeeruddin and M. Grätzel, *Energy Environ. Sci.*, 2011, **4**, 842; (*d*) Y. Yen, H. Chou, Y. Chen, C. Hsu and J. T. Lin, *J. Mater. Chem.*, 2012, **22**, 8734; (*e*) M. Liang and J. Chen, *Chem. Soc. Rev.*, 2013, **42**, 3453. (f) Y. Z. Wu and W. H. Zhu, *Chem. Soc. Rev.*, 2013, **42**, 2039.
4 B. Chen, D. Chen, C. Chen, C. Hsu, H. Hsu, K. Wu, S. Liu, P. Chou and Y. Chi, *J. Mater. Chem.*, 2011, **21**, 1937.
5 (*a*) S. Mathew, A. Yella, P. Gao, R. Humphry-Baker, F. E. CurchodBasile, N. Ashari-Astani, I. Tavernelli, U. Rothlisberger, M. K. Nazeeruddin and M. Grätzel, *Nat. Chem.*, 2014, **6**, 242; (*b*) K. Kakiage, Y. Aoyama, T. Yano, T. Otsuka, T. Kyomen, M. Unno and M. Hanaya, *Chem. Commun.*, 2014, **50**, 6379; (*c*) Z. Yao, M. Zhang, H. Wu, L. Yang, R. Li and P. Wang, *J. Am. Chem. Soc.*, 2015, **137**, 3799; (*d*) N. Zhou, K. Prabakaran, B. Lee, S. H. Chang, B. Harutyunyan, P. Guo, M. R. Butler, A. Timalsina, M. J. Bedzyk, M. A. Ratner, S. Vegiraju, S. Yau, C. Wu, R. P. H. Chang, A. Facchetti, M. Chen and T. J. Marks, *J. Am. Chem. Soc.*, 2015, **137**, 4414.
6 (*a*) P. Gao, H. N. Tsao, M. Grätzel and M. K. Nazeeruddin, *Org. Lett.*, 2012, **14**, 4330; (*b*) R. Yeh-Yung Lin, H. Lin, Y. Yen, C. Chang, H. Chou, P. Chen, C. Hsu, Y. Chen, J. T. Lin and K. Ho, *Energy Environ. Sci.*, 2013, **6**, 2477; (*c*) K. M. Karlsson, X. Jiang, S. K. Eriksson, E. Gabrielsson, H. Rensmo, A. Hagfeldt and L. Sun, *Chem. Eur. J.*, 2011, **17**, 6415; (*d*) H. Choi, M. Shin, K. Song, M. Kang, Y. Kang and J. Ko, *J. Mater. Chem. A*, 2014, **2**, 12931; (*e*) X. Hao, M. Liang, X. Cheng, X. Pian, Z. Sun and S. Xue, *Org. Lett.*, 2011, **13**, 5424; (*f*) E. Kozma, I. Concina, A. Braga, L. Borgese, L. E. Depero, A. Vomiero, G. Sberveglieri and M. Catellani, *J. Mater. Chem.*, 2011, **21**, 13785; (*g*) L. Tan, J. Huang, Y. Shen, L. Xiao, J. Liu, D. Kuang and C. Su, *J. Mater. Chem. A*, 2014, **2**, 8988.
7 (*a*) H. Shang, K. Jiang and X. Zhan, *Org. Electron.*, 2012, **13**, 2395; (*b*) J. H. Zhao, X. C. Yang, M. Cheng, S. F. Li and L. C. Sun. *J. Phys. Chem. C*, 2013, **117**, 12936; (*c*) A. L. Capodilupo, L. De Marco, E. Fabiano, R. Giannuzzi, A. Scrascia, C. Clarlucci, G. A. Corrente, M. P. Cipolla, G. Gigli and G. Ciccarella, *J. Mater. Chem. A*, 2014, **2**, 14181; (*d*) H. J. Jo, J. E. Nam, D. H. Kim, H. Kim and J. K. Kang, *Dyes Pigments*, 2014, **102**, 285; (*e*) M. Lee, J. Kim, D. Lee and M. J. Ko, *ACS Appl. Mater. Interfaces*, 2014, **6**, 4102; (*f*) C. Teng, X. C. Yang, C. Yang, H. N. Tian, S. F. Li, X. N. Wang, A. Hagfeldt and L. C. Sun, *J. Phys. Chem. C*, 2010, **114**, 11305; (*g*) K. D. Seo, H. M. Song, M. J. Lee, M. Pastore, C. Anselmi, F. D. Angelis, M. K. Nazeeruddin, M. Grätzel and H. K. Kim, *Dyes Pigments*, 2011, **90**, 304; (*h*) H. Kim and H. S. Freeman, *J. Mater. Chem.*, 2012, **22**, 20403; (*i*) M. Z. Yigit, H. Bilgili, E. Sefer, S. Demin, C. Zafer, M. Can and S. Koyuncu, *Electrochim. Acta*, 2014, **147**, 617.
8 (*a*) C. Hsieh, H. Lu, C. Chiu, C. Lee, S. Chuang, C. Mai, W. Yen, S. Hsu, E. W. Diau and C. Yeh, *J. Mater. Chem.*, 2010, **20**, 1127; (*b*) Y. Hong, J. Liao, D. Cao, X. Zang, D. Kuang, L. Wang, H. Meier and C. Su, *J. Org. Chem.*, 2011, **76**, 8015; (*c*) B. Liu, W. Wu, X. Li, L. Li, S. Guo, X. Wei, W. Zhu and Q. Liu, *Phys. Chem. Chem. Phys.*, 2011, **13**, 8985; (*d*) Z. Wan, C. Jia, Y. Duan, L. Zhou, Y. Lin and Y. Shi, *J. Mater. Chem.*, 2012, **22**, 25140; (*e*) J. Shi, Z. Chai, C. Zhong, W. Wu, J. Hua, Y. Dong, J. Qin, Q. Li and Z. Li, *Dyes Pigments*, 2012, **95**, 244; (*f*) W. Ying, J. Yang, M. Wielopolski, T. Moehl, J. Moser, P. Comte, J. Hua, S. M. Zakeeruddin, H. Tian and M. Grätzel, *Chem. Sci.*, 2014, **5**, 206; (*g*) C. Luo, W. Bi, S. Deng, J. Zhang, S. Chen, B. Li, Q. Liu, H. Peng and J. Chu, *J. Phys. Chem. C*, 2014, **118**, 14211; (h) D. Casanova, *ChemPhysChem*, 2011, **12**, 2979; (i) T. W. Holcombe, J. Yum, J. Yoon, P. Gao, M. Marszalek, D. D. Censo, K. Rakstys, M. K. Nazeeruddin and M. Gräetzel, *Chem. Commun.*, 2012, **48**, 10724.
9 K. Pei, Y. Z. Wu, W. J. Wu, Q. Zhang, B. Q. Chen, H. Tian and W. H. Zhu, *Chem. Eur. J.*, 2012, **18**, 8190.
10 K. Pei, Y. Z. Wu, A. Islam, Q. Zhang, L. Y. Han, H. Tian and W. H. Zhu, *ACS Appl. Mater. Interfaces*, 2013, **5**, 4986.
11 K. Pei, Y. Z. Wu, A. Islam, S. Q. Zhu, L. Y. Han, Z. Y. Geng and W. H. Zhu, *J. Phys. Chem. C*, 2014, **118**, 16552.
12 J. Yang, P. Ganesan, J. Teuscher, T. Moehl, Y. J. Kim, C. Yi, P. Comte, K. Pei, T. W. Holcombe, M. K. Nazeeruddin, J. Hua, S. M. Zakeeruddin, H. Tian and M. Grätzel, *J. Am. Chem. Soc.*, 2014, **136**, 5722.
13 S. Ito, T. N. Murakami, P. Comte, P. Liska, C. Grätzel, M. K. Nazeeruddin and M. Grätzel, *Thin Solid Films*, 2008, **516**, 4613.
14 G. Schlichthörl, S. Y. Huang, J. Sprague and A. J. Frank, *J. Phys. Chem. B*, 1997, **101**, 8141.
15 N. W. Duffy, L. M. Peter, R. M. G. Rajapakse and K. G. U. Wijayantha, *J. Phys. Chem. B*, 2000, **104**, 8916.
16 R. Scaria, S. K. Dhawan and S. Chand, *Syn. Met.*, 2014, **191**, 168.
17 L. I. Belen'kii, V. Z. Shirinyan, G. P. Gromova, A. V. Kolotaev, Y. A. Strelenko, S. N. Tandura, A. N. Shumskii and M. M. Krayushkin, *Chem. Heterocycl. Compd.*, 2003, **39**, 1570.
18 O. Miyata, N. Takeda, Y. Kimura, Y. Takemoto, N. Tohnai, M. Miyata and T. Naito, *Tetrahedron*, 2006, **62**, 3629.
19 W. H. Zhu, Y. Z. Wu, S. T. Wang, W. Q. Li, X. Li, J. Chen, Z. S. Wang and H. Tian, *Adv. Funct. Mater.*, 2011, **21**, 756.
20 M. J. Frisch, G. W. Trucks, H. B. Schlegel, G. E. Scuseria, M. A. Robb, J. R. Cheeseman, G. Scalmani, V. Barone, B. Mennucci, G. A. Petersson, H. Nakatsuji, M. Caricato, X. Li, H. P. Hratchian, A. F. Izmaylov, J. Bloino, G. Zheng, J. L. Sonnenberg, M. Hada, M. Ehara, K. Toyota, R. Fukuda, J. Hasegawa, M. Ishida, T. Nakajima, Y. Honda, O. Kitao, H. Nakai, T. Vreven, J. A. Montgomery, J. E. Peralta, F. Ogliaro, M. Bearpark, J. J. Heyd, E. Brothers, K. N. Kudin, V. N. Staroverov, R. Kobayashi, J. Normand, K. Raghavachari, A. Rendell, J. C. Burant, S. S. Iyengar, J. Tomasi, M. Cossi, N. Rega, J. M. Millam, M. Klene, J. E. Knox, J. B. Cross, V. Bakken, C. Adamo, J. Jaramillo, R. Gomperts, R. E. Stratmann, O. Yazyev, A. J. Austin, R. Cammi, C. Pomelli, J. W. Ochterski, R. L. Martin, K. Morokuma, V. G. Zakrzewski, G. A. Voth, P. Salvador, J. J. Dannenberg, S. Dapprich, A. D. Daniels, O. Farkas, J. B. Foresman, J. V. Ortiz, J. Cioslowski and D. J. Fox, *Gaussian 09*, Revision A.02, Gaussian, Inc., Wallingford CT, **2009**.
21 S. H. Jiang, X. F. Lu, G. Zhou and Z.-S. Wang, *Chem. Commun.*, 2013, **49**, 3899.
22 L. Yang, Z. W. Zheng, Y. Li, W. J. Wu, H. Tian and Z. H. Wang, *Chem. Commun.*, 2015, **51**, 4842.

D-A-π-A featured sensitizers by modification of auxiliary acceptor for preventing "trade-off" effect†

Haibo Zhu, Bo Liu,* Jingchuan Liu, Weiwei Zhang, and Wei-Hong Zhu*

The two grafted thiophene groups onto the auxiliary quinoxaline acceptor successfully overcome the unfavorable "trade-off" effect between photocurrent and photovoltage.